TÜBİTAK

Turkish Journal of Chemistry

http://journals.tubitak.gov.tr/chem/

Research Article

Turk J Chem
(2013) 37: 775 – 795

doi:10.3906/kim-1303-28

Synthesis, spectroscopic characterization, and biological screening of binuclear transition metal complexes of bicompartmental Schiff bases containing indole and resorcinol moieties

Mahendra Raj KAREKAL, Mruthyunjayaswamy BENNIKALLU HIRE MATHADA*
Department of Studies and Research in Chemistry, Gulbarga University, Gulbarga, Karnataka, India

Received: 11.03.2013 • **Accepted:** 13.04.2013 • **Published Online:** 16.09.2013 • **Printed:** 21.10.2013

Abstract: A series of binucleating Cu(II), Ni(II), and Zn(II) complexes of bicompartmental ligands with ONO donors were prepared. The ligands were synthesized by the condensation of 5-substituted-3-phenyl-1 *H* -indole-2-carboxyhydrazides and 4,6-diacetylresorcinol. The newly synthesized ligands and their complexes were characterized by elemental analysis and various spectral studies like IR, ^{1}H NMR, ESI-mass, UV-Vis, ESR, thermal studies, magnetic susceptibility, molar conductance, and powder-XRD data. All the complexes were binuclear and monomeric in nature. Cu(II) complexes have octahedral geometry, whereas Ni(II) and Zn(II) complexes have square planar and tetrahedral geometry, respectively. The redox property of the Cu(II) complex was investigated by electrochemical method using cyclic voltammetry. In order to evaluate the effect of metal ions upon chelation, both the ligands and their metal complexes were screened for their antibacterial and antifungal activities by minimum inhibitory concentration (MIC) method. The DNA cleaving capacity of all the complexes was analyzed by agarose gel electrophoresis.

Key words: Indole Schiff bases, binuclear complexes, electrochemical, antimicrobial, DNA cleavage

1. Introduction

The indole structure represents a highly relevant heterocyclic system, since large numbers of indole-containing synthetic and natural products such as vincristine, indole-micine, reserpine, mitomycin, dolasetron mesylate, pindolol, indomethacin, and sumatriptan are being used as vital drugs in the treatment of various illnesses. Large numbers of pharmacological compounds that contain indole nuclei have been reported to possess various biological properties, viz., anti-inflammatory,[1−3] anticonvulsant,[4] antibacterial,[5] COX-2 inhibitory,[6,7] and antiviral activities.[8] There are several reports that have described that indole-2-carbohydrazides and related compounds exhibited MAO inhibitory,[9,10] antihistaminic,[11] and antidepressant activities.[12]

The difunctional carbonyl compound 4,6-diacetylresorcinol acts as a precursor for the formation of various binucleating ligands[13−15] and it is used as primary ligand in the synthesis of various mixed-ligand complexes.[16,17] Difunctional 4,6-diacetylresorcinol is also employed in the construction of ligands containing ONS donors by its condensation with various thiosemicarbazides and thiocarbohydrazides.[18] The ligands synthesized by the difunctional carbonyl compound are used to synthesize mono-, bi-, and poly-nuclear complexes with different binding modes and their structural and functional features were explored in the development of many biologically active compounds. Studies on binuclear metal complexes have stimulated interest owing

*Correspondence: bhmmswamy53@rediffmail.com

to their unique physicochemical properties. These types of complexes have contributed to a better knowledge of oxygen transport and activation by metalloenzymes such as hemocyanin (Cu_2) and cytochrome-C-oxidase (CuFe)[19] as well as of some industrial catalytic processes.[20] Deoxyribonucleic acid (DNA) is the primary target molecule for most antiviral therapies. Small molecule interactions with DNA continue to be intensely and widely studied for their usefulness as probes of cellular replication and transcriptional regulation and for their potential pharmaceutical properties. The ability of metallodrugs to bring about DNA-cleavage is an important criterion in the development of metallodrugs as active chemotherapeutic agents. A number of transition metal complexes showed DNA-cleavage because of their redox behavior. In this study, 4,6-diacetylresorcinol was selected as precursor for the construction of bicompartmental ligands. In spite of the extensive scientific literature on Schiff base metal complexes with indole moiety, not much is known about bicompartmental Schiff bases derived from indole moiety and their metal complexes. In view of these findings and in continuation of our research work on pharmaceutically active indole molecules,[21–24] we report herein the synthesis, characterization, and biological evaluation studies of 5-substituted-3-phenyl-1*H*-indole-2-carboxyhydrazides Schiff bases obtained by the condensation of 5-substituted-3-phenyl-1*H*-indole-2-carboxyhydrazides and 4,6-diacetylresorcinol and their metal complexes in order to obtain new classes of biologically active compounds.

2. Results and discussion

All the synthesized metal complexes are colored solids, amorphous in nature and stable in air. Melting points of the newly synthesized metal complexes were above 300 °C. The complexes are insoluble in water and common organic solvents but are soluble in strong coordinating solvents like DMF and DMSO. Elemental analysis and analytical data of the complexes (Table 1) suggest that the metal to ligand ratio of the complexes is 2:1 stoichiometry of the type $[M_2(L)(Cl)_2(H_2O)_4]$ for Cu(II) complexes and $[M_2(L)(Cl)_2]$ for Ni(II) and Zn(II) complexes of both ligands (**1** and **2**), where L stands for deprotonated ligand. The molar conductance values are too low to account for any dissociation of the complexes in DMF (25.23–41.44 Ω^{-1} cm^2 mol^{-1}), indicating the nonelectrolytic nature of the complexes in DMF.[25]

2.1. IR spectral data

The important IR bands of the ligands and their metal complexes are represented in Table 2. In the IR spectra of ligands **1** and **2,** absorption due to phenolic OH exhibited bands at 3406 and 3416 cm^{-1}, while absorption due to indole NH and CONH functions displayed bands at 3285 and 3184 cm^{-1} and 3258 and 3142 cm^{-1}, respectively. The phenolic C-O function of ligands **1** and **2** displayed absorption bands at 1233 and 1236 cm^{-1}, respectively. In both ligands, absorption bands due to carbonyl and azomethine functions appeared at 1657 and 1601 cm^{-1} and 1651 and 1542 cm^{-1}, respectively.

The absence of absorption bands due to phenolic OH groups at 3406 and 3416 cm^{-1} in the IR spectra of Cu(II), Ni(II), and Zn(II) complexes of ligands **1** and **2** indicates the formation of bonds between metal ion and phenolic oxygen atom via deprotonation. This is further confirmed by the increase in absorption frequency of phenolic C-O, which appeared in the region 1258–1271 cm^{-1} and 1258–264 cm^{-1}, respectively, in the metal complexes of both ligands in the present study. The absorption due to indole NH and CONH functions of the above metal complexes of ligands **1** and **2** displayed bands in the region 3286–3278 cm^{-1} and 3178–3170 cm^{-1} and 3261–3242 cm^{-1} and 3157–3142 cm^{-1} respectively, which appeared in about the same region as in the case of the respective ligands, thus confirming the noninvolvement of either indole NH or CONH function in coordination with the metal ions. The absorption frequency of carbonyl and azomethine functions, which

Table 1. Physical, analytical, and magnetic susceptibility data of ligands 1 and 2 and their complexes.

Ligand/complexes		Molecular formula	Mol. wt.	Elemental analysis (%) Calcd (Found)					Mag. moment		Color
				M	C	H	N	Cl	μ^{a}_{total} (BM)	μ^{b}_{eff} (BM)	
1	H_2L_1	$C_{40}H_{30}N_6O_4Cl_2$	728	–	65.93 (65.91)	4.12 (4.09)	11.53 (11.50)	9.61 (9.59)	–	–	Pale yellow
1a	$[Cu_2(L_1)(Cl)_2(H_2O)_4]$	$Cu_2[C_{40}H_{36}N_6O_8Cl_4]$	995.08	12.77 (12.71)	48.23 (48.20)	3.61 (3.58)	8.44 (8.41)	14.06 (14.01)	2.66	1.51	Green
1b	$[Ni_2(L_1)(Cl)_2]$	$Ni_2[C_{40}H_{28}N_6O_4Cl_4]$	913.38	12.85 (12.82)	52.55 (52.51)	3.06 (3.02)	9.19 (9.17)	15.32 (15.28)	Dia mag	Dia mag	Brown
1c	$[Zn_2(L_1)(Cl)_2]$	$Zn_2[C_{40}H_{28}N_6O_4Cl_4]$	926.78	14.11 (14.09)	51.79 (51.72)	3.02 (3.00)	9.06 (9.01)	15.10 (15.07)	Dia mag	Dia mag	Yellowish orange
2	H_2L_2	$C_{42}H_{36}N_6O_4$	688	-	73.25 (73.21)	5.23 (5.19)	12.20 (12.17)	–	–	–	Pale yellow
2a	$[Cu_2(L_2)(Cl)_2(H_2O)_4]$	$Cu_2[C_{42}H_{42}N_6O_8Cl_2]$	955.08	13.30 (13.24)	52.77 (52.74)	4.39 (4.32)	8.79 (8.74)	7.32 (7.28)	2.68	1.52	Green
2b	$[Ni_2(L_2)(Cl)_2]$	$Ni_2[C_{42}H_{34}N_6O_4Cl_2]$	873.38	13.43 (13.40)	57.70 (57.65)	3.89 (3.82)	9.61 (9.58)	8.01 (7.96)	Dia mag	Dia mag	Light brown
2c	$[Zn_2(L_2)(Cl)_2]$	$Zn_2[C_{42}H_{34}N_6O_4Cl_2]$	886.78	14.74 (14.70)	56.83 (56.80)	3.83 (3.81)	9.47 (9.43)	7.89 (7.83)	Dia mag	Dia mag	Orange

[a]μ total the total magnetic moment of the complex.
[b]μ eff where calculated for one metal ion in the complex.

Table 2. IR spectral data of ligands **1** and **2** and their complexes.

Ligands/complexes		ν_{OH}	ν_{H2O}	NH (indole)	NH (amide)	C=O (carbonyl)	C=N (azomethine)	C-O (phenolic)	M-O	M-N	M-Cl
1	H_2L_1	3406	-	3285	3184	1657	1601	1233	-	-	-
1a	$[Cu_2(L_1)(Cl)_2(H_2O)_4]$	-	3414	3281	3171	1633	1584	1271	540	470	273
1b	$[Ni_2(L_1)(Cl)_2]$	-	-	3286	3170	1614	1585	1261	590	439	285
1c	$[Zn_2(L_1)(Cl)_2]$	-	-	3278	3178	1633	1585	1258	509	462	266
2	H_2L_2	3416	-	3258	3142	1651	1542	1236	-	-	-
2a	$[Cu_2(L_2)(Cl)_2(H_2O)_4]$	-	3400	3246	3157	1628	1518	1258	590	470	289
2b	$[Ni_2(L_2)(Cl)_2]$	-	-	3242	3143	1614	1536	1264	536	439	289
2c	$[Zn_2(L_2)(Cl)_2]$	-	-	3261	3142	1629	1538	1259	555	493	293

appeared at 1657 and 1601 cm^{-1} and 1651 and 1542 cm^{-1} in the case of ligands **1** and **2**, respectively, shifted to lower frequency by 43–24 and 17–16 cm^{-1} and 37–22 and 24–4 cm^{-1}, respectively, in the complexes and appeared in the region 1633–1614 and 1585–1584 cm^{-1} and 1629–1614 and 1538–1518 cm^{-1}, indicating the involvement of the oxygen atom of carbonyl function as such without undergoing any enolization[26] and the nitrogen atom of azomethine[27] function in complexation with the metal ions. This is further confirmed by the appearance of new bands in the region 590–509 and 470–439 cm^{-1} and 590–536 and 493–439 cm^{-1} due to M-O and M-N stretching vibrations[28] in all the complexes of ligands **1** and **2**, respectively. The appearance of new bands in the region 285–266 and 293–289 cm^{-1} in all the synthesized complexes was due to M-Cl bands. The broad band due to the coordinated water molecule appeared at 3414 and 3400 cm^{-1} in the Cu(II) complexes of ligands **1** and **2**, respectively.

2.2. ^{1}H NMR spectral data

The ^{1}H NMR data of ligands **1** and **2** and their Zn(II) complexes are presented in Table 3. The ^{1}H NMR spectra of ligands **1** (Figure 1) and **2** displayed singlets each at 12.62, 12.29, and 10.48 ppm and 12.62, 12.25, and 10.25, ppm respectively, due to the 2 protons of amide NH, 2 protons of indole NH, and 2 OH protons of ligands **1** and **2**, respectively. The aromatic protons of ligands **1** and **2** resonated as multiplets in the region 6.35–7.57 ppm (m, 18H, ArH) and 6.35–7.55 ppm (m, 18H, ArH). Six protons of 2 methyl groups attached to azomethine carbon atoms resonated as distinct singlets at 2.02 ppm and 1.99 ppm, respectively. Six protons of 2 methyl groups attached to the 5-position of 2 indole moieties of ligand **2** appeared as a distinct singlet at 2.63 ppm.

Table 3. ^{1}H NMR data of Zn(II) complexes of ligands **1** and **2**.

Ligands/Zn(II) complexes		^{1}H NMR data (ppm)
1	(H_2L_1)	12.62 (s, 2H, 2 CONH), 12.29 (s, 2H, 2 indole NH), 10.48 (s, 2H, 2 phenolic OH), 6.35–7.57 (m, 18H, ArH), 2.02 (s, 6H, 2 CH_3)
1c	$[Zn_2(L_1)(Cl)_2]$	12.63 (s, 2H, 2 CONH), 12.39 (s, 2H, 2 indole NH), 6.36–7.97 (m, 18H, ArH), 2.03 (s, 6H, 2 CH_3)
2	(H_2L_2)	12.62 (s, 2H, 2 CONH), 12.25 (s, 2H, 2 indole NH), 10.25 (s, 2H, 2 phenolic OH), 6.35–7.55 (m, 18H, ArH), 2.63 (s, 6H, 2 CH_3), 1.99 (s, 6H, 2 CH_3)
2c	$[Zn_2(L_2)(Cl)_2]$	12.69 (s, 2H, 2 CONH), 12.30 (s, 2H, 2 indole NH), 7.04–8.07 (m, 18H, ArH), 2.68 (s, 6H, 2 CH_3), 2.00 (s, 6H, 2 CH_3)

In the case of Zn(II) complexes, the absence of a signal due to the proton of 2 phenolic OH groups confirms the involvement of bonding of the phenolic oxygen atom to the metal ion via deprotonation. The signals at 12.63 and 12.69 ppm, 12.39 and 12.30 ppm, 6.36–7.97 and 7.04–8.07 ppm, and 2.03 and 2.00 ppm are due to 2 amide NH protons, 2 indole NH protons, aromatic protons, and 6 protons of 2 methyl groups attached to 2 azomethine carbon atoms in each of Zn(II) complexes of ligands **1** and **2**, respectively. The singlet that appeared at 2.68 ppm in the case of the Zn(II) complex of ligand **2** is due to 6 protons of 2 methyl groups attached to the 5-position of the indole moiety. A considerable degree of symmetry is present in these compounds so that the protons in the 2 halves of the molecules are magnetically equivalent. When compared to the ^{1}H NMR spectra of ligands **1** and **2** and their Zn(II) complexes, all the signals due to protons shifted downfield, confirming the complexation of Zn(II) ions with the ligands. Thus the ^{1}H NMR data support the assigned structures.

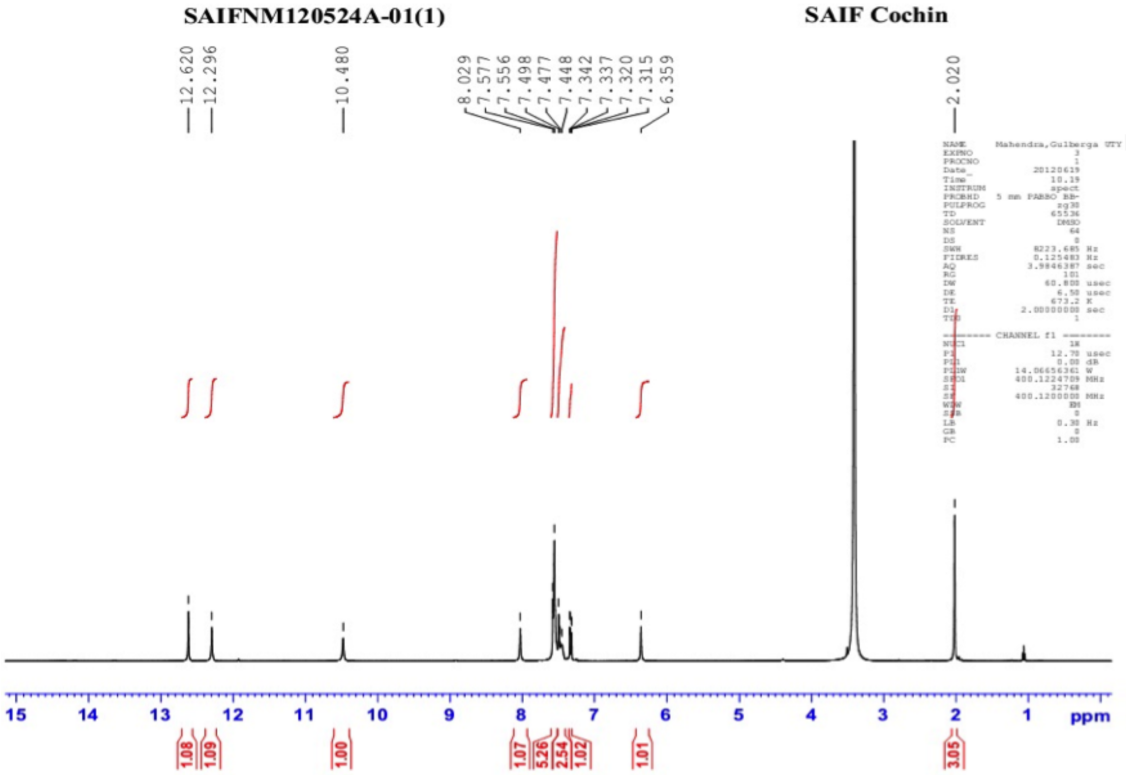

Figure 1. ^{1}H NMR spectrum of ligand 1.

2.3. ESI-mass spectral data

Ligand **1** and its Cu(II), Ni(II), and Zn(II) complexes were studied for their mass spectra. The ESI-mass spectra of ligand **1** and its Cu(II), Ni(II), and Zn(II) complexes exhibited molecular ion peaks equivalent of their molecular weight along with other fragmentation peaks. The representative mass spectrum of ligand **1** showed a molecular ion peak due to $M^{+}1$ at m/z 729, 731, 733 (20%, 6%, 2.2%). This on loss of hydrogen radical gave a peak at m/z 728, 730, 732 (10%, 3.2%, 9%), which is equivalent to its molecular weight. Further, simultaneous loss of $C_{17}H_{13}N_3OCl$ radical, OH radical, and H radical gave a fragment ion peak at 400, 402 (100%, 33.3%), which is also a base peak. This fragmentation pattern (Scheme 1) is consistent with its structure.

The ESI-mass spectrum of Cu(II) complex (**1a**) (Figure 2) of ligand **1** exhibited a molecular ion peak at $M^{+}1$ 995, 997, 999 (21%, 7.2%, 2.3%) which corresponds to its molecular weight, which on loss of 2 water molecules and a CH_3 radical gave a fragment ion peak recorded at m/z 944, 946, 948 (60%, 32.8%, 6.6%), which on simultaneous loss of 2 water molecules, chloride radical, chlorine molecule, and 5-chloro-3-pheny-indole-2-yl radical gave a fragment ion peak recorded at m/z 577 (10.3%). This on further loss of C_4H_3 radical, CO molecule, CH_3 radical, 1 hydrogen molecule, and 2 hydrogen radicals gave a fragment ion peak recorded at m/z 479 (100%), which is also a base peak. This fragmentation pattern (Scheme 2) is in conformity with the structure of the complex.

Similarly, the mass spectra of Ni(II) and Zn(II) complexes of ligand **1** exhibited a molecular ion peak at $M^{+}1$ 913, 915, 917 (17%, 5.83%, 1.8%) and 926, 928, 930 (31.2%, 10.4%, 3.46%), which corresponds to their molecular weight. The fragmentation pattern of both complexes is depicted in Schemes 3 and 4, respectively.

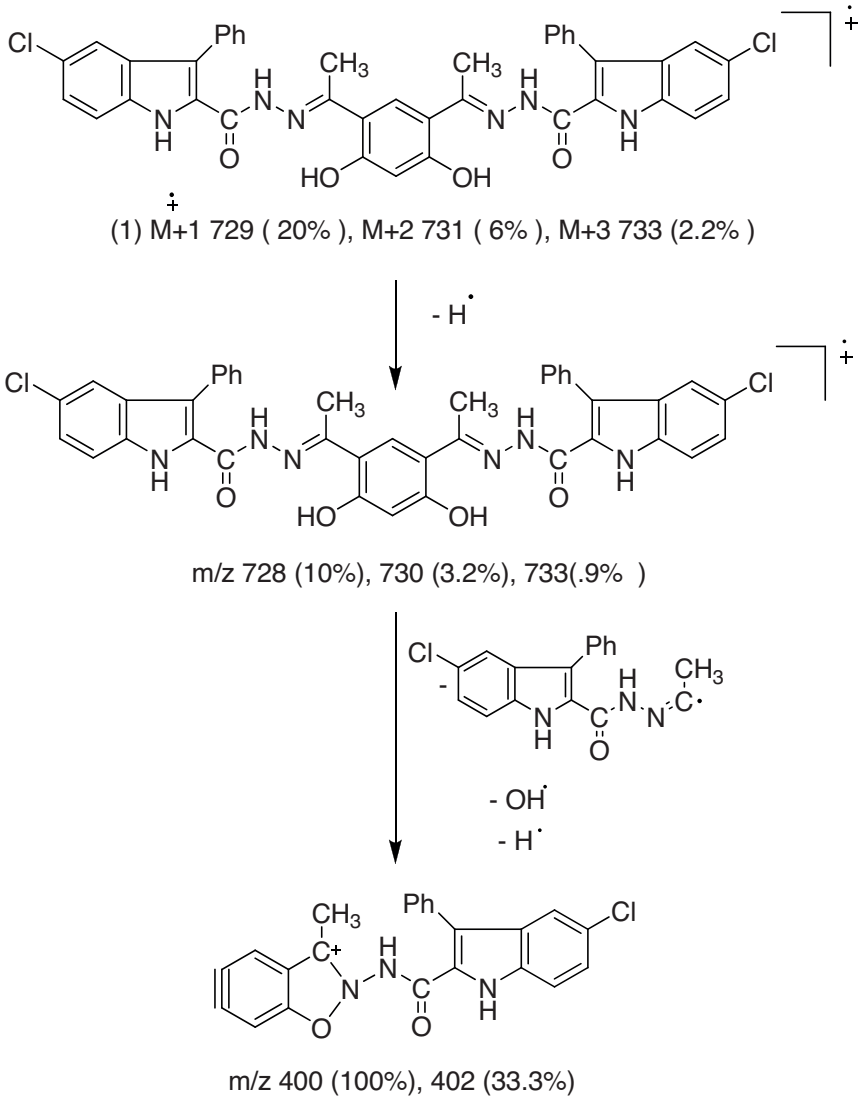

Scheme 1. Fragmentation pattern of ligand **1**.

2.4. Electronic spectral and magnetic susceptibility data

The electronic absorption spectra of Cu(II) and Ni(II) complexes of ligands **1** and **2** were recorded in distilled DMF (10^{-3} M) at room temperature. The band positions of absorption band maxima assignments are listed in Table 4. The electronic spectra of the Cu(II) complexes of ligands **1** and **2** showed 1 low intensity broad band and 1 high intensity band each around 627.27 (15,942.10 cm^{-1}) and 393.34 (25,423.30 cm^{-1}) nm and 630.25 (15,866.72 cm^{-1}) and 392.88 (25,453.06 cm^{-1}) nm, respectively. The low intensity broad band is assignable to $^2T_{2g} \leftarrow 2E_g$ transition and the high intensity band observed is due to symmetry forbidden ligand $\rightarrow$ metal charge transfer. Based on the electronic spectral data, distorted octahedral geometry around Cu(II) ion is suggested.[29,30] This was further supported by their magnetic susceptibility measurements. The total magnetic moment values (μ_{Total}) of Cu(II) complexes of ligands **1** and **2** are 2.66 and 2.68, respectively. The calculated μ_{eff} value for each Cu(II) complex is 1.51 and 1.52 (magnetic moment for 1 metal ion) due to the 2 adjacent

Cu(II) ions having 1 electron each possessing an antiferromagnetic interaction between them. Thus, based on the above data, these Cu(II) ions achieve octahedral geometry by the addition of 2 water molecules[31] and this was further confirmed by the thermal studies.

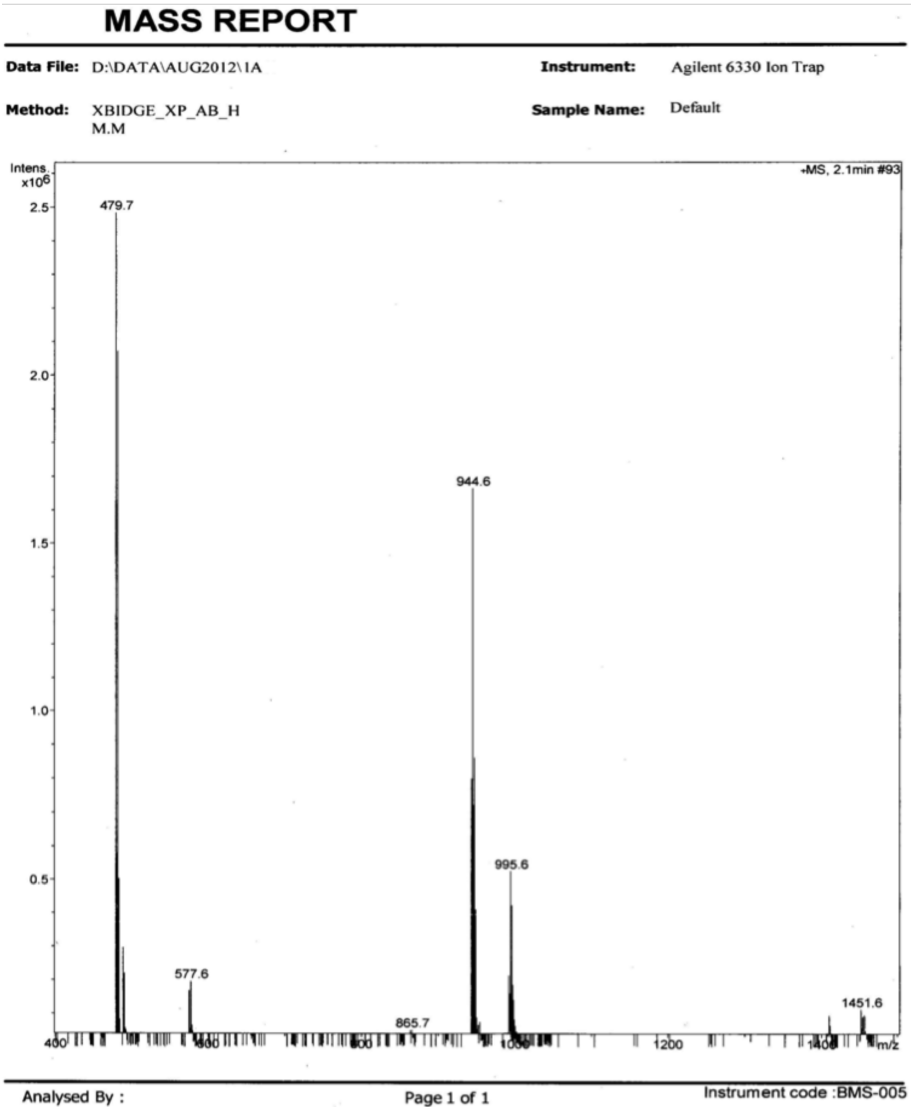

Figure 2. ESI-mass spectrum of Cu(II) complex **(1a)**.

The electronic spectra of the Ni(II) complexes of ligands **1** and **2** displayed 2 bands each at 710.0 (14,084.51 cm^{-1}) and 460.0 (21,739.13 cm^{-1}) nm and 710.80 (14,068.66 cm^{-1}) and 460.60 (21,710.81 cm^{-1}) nm, which are assignable to $^1A_{1g} \rightarrow {}^1E_g$ and $^1A_{1g} \rightarrow {}^1B_{2g}$ transitions, respectively. Since these complexes are diamagnetic in nature, a square-planar geometry is suggested for the Ni(II) complexes.[32,33]

2.5. ESR spectral studies of the Cu(II) complexes of ligands 1 and 2

To obtain information about the hyperfine and superhyperfine structure in order to elucidate the geometry of the complex and the site of the metal–ligand bonding or environment around the metal ion the X-band ESR

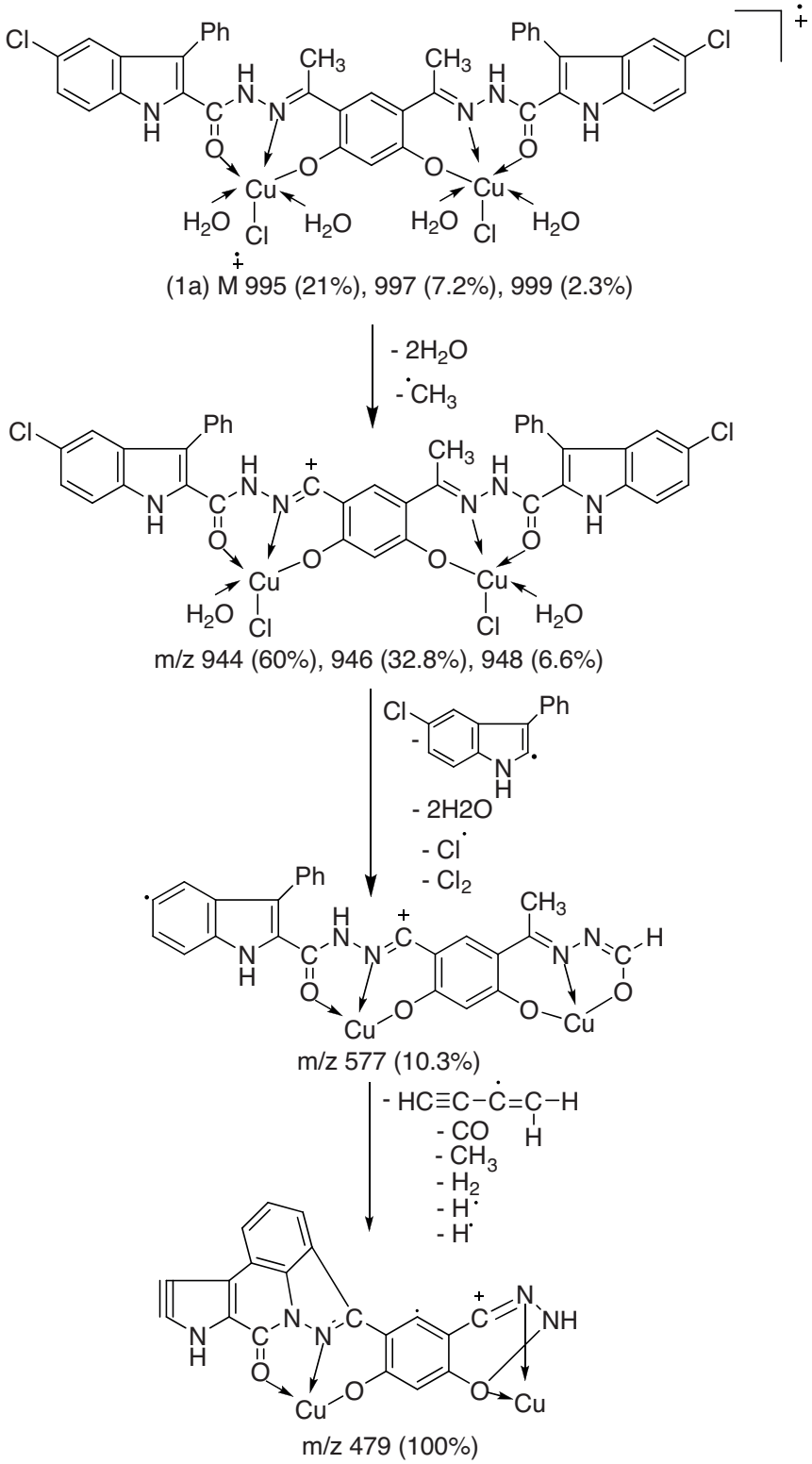

Scheme 2. Fragmentation pattern of Cu(II) complex (**1a**).

spectra of Cu(II) complexes $[Cu_2(L_1)(Cl)_2(H_2O)_4]$ (**1a**) and $[Cu_2(L_2)(Cl)_2(H_2O)_4]$ (**2a**) were recorded in the polycrystalline state at room temperature at a frequency of 9.387 GHz with a field set of 3950 G and the spectral data are given in Table 4. The spin Hamiltonian parameters for the Cu(II) complex were used to derive the ground state. In octahedral geometry, for the g-tensor parameter with $g_{||} > g_{\perp} > 2.0023$, the unpaired electron lies in the d_{x2-y2} orbital in ground state and with $g_{\perp} > g_{||} > 2.0023$, the unpaired electron lies in

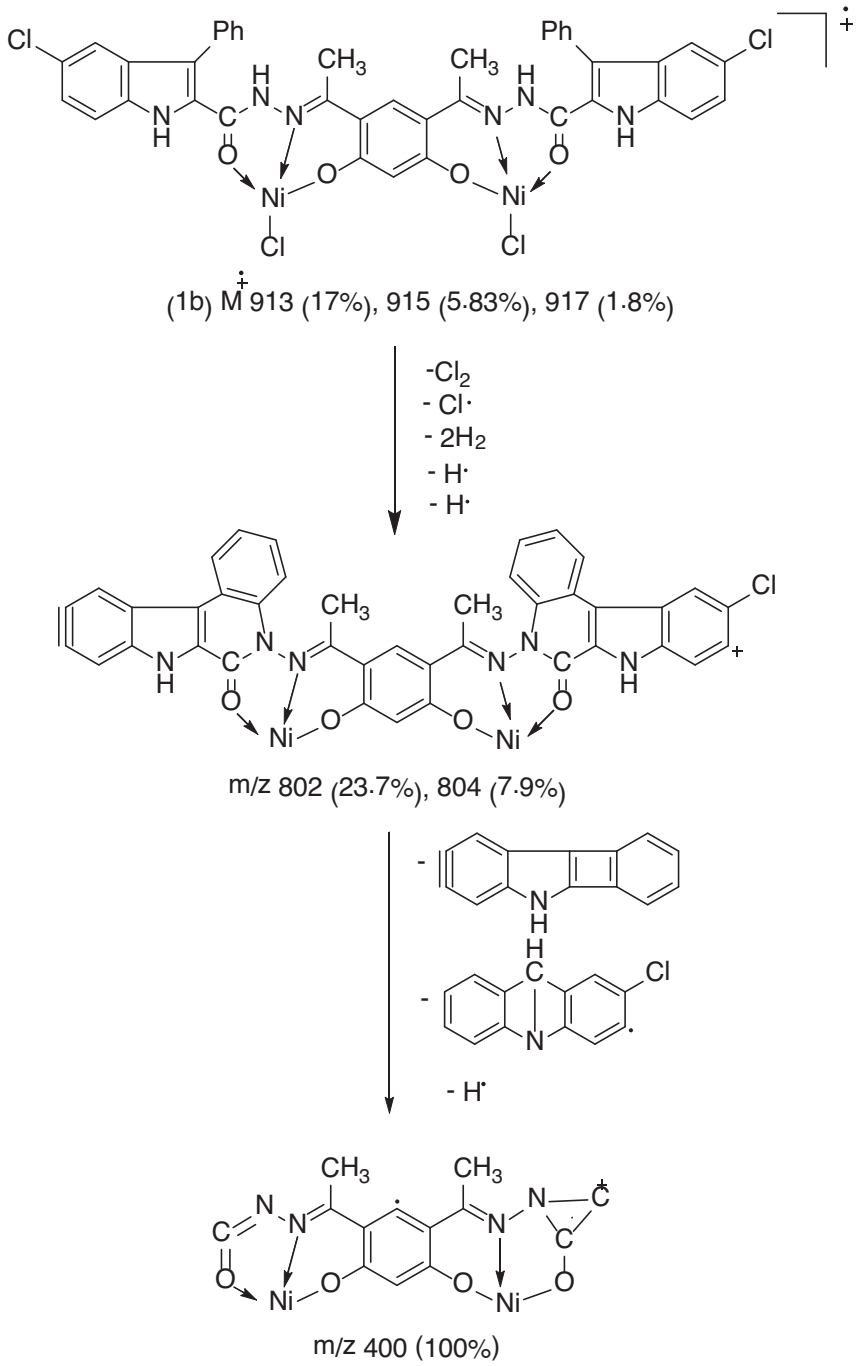

Scheme 3. Fragmentation pattern of Ni(II) complex (**1b**).

the d_z^2 orbital.[34] The observed measurements for Cu(II) complexes, $[Cu_2(L_1)(Cl)_2(H_2O)_4]$ (**1a**), $g_{||}$ (2.43) $> g_\perp$ (2.39) $>$ 2.0023 and $[Cu_2(L_2)(Cl)_2(H_2O)_4]$ (**1b**), $g_{||}$ (2.44) $> g_\perp$ (2.32) $>$ 2.0023, indicate that the complexes are axially symmetric and the copper site has a d_{x2-y2} ground state characteristic of octahedral geometry for both complexes.[35] The $g_{||}$ value is an important function for indicating the covalent character of metal–ligand bond, for ionic $g_{||} < 2.3$ and for covalent characters $g_{||} > 2.3$, respectively.[36] In the present Cu(II) complexes the $g_{||}$ values are more than 2.3, indicating an appreciable covalent character for the metal–ligand bond. The geometric parameter (G), which is the measure of extent of exchange interaction, is calculated by

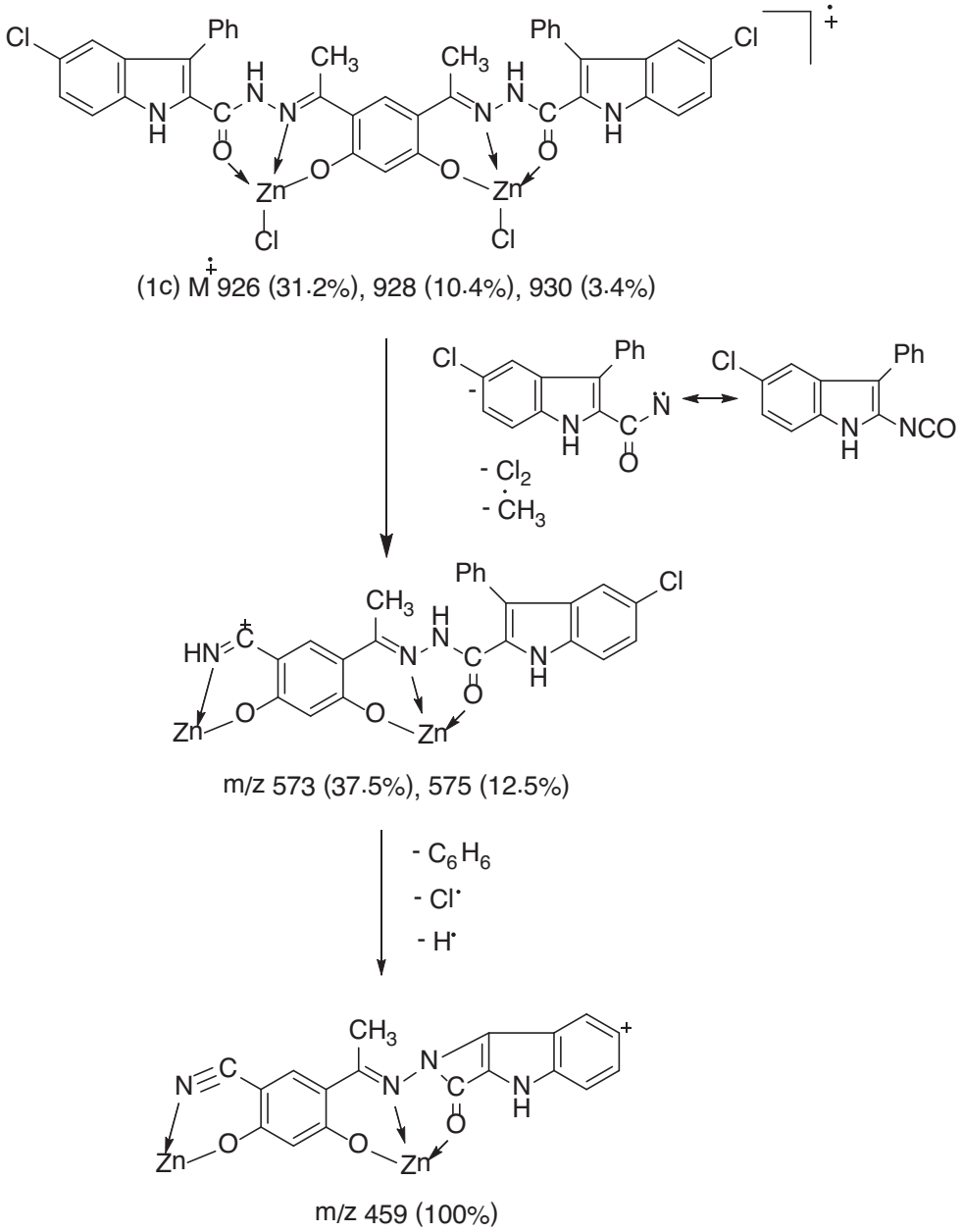

Scheme 4. Fragmentation pattern of Zn(II) complex (**1c**).

using g-tensor values by the expression $G = g_{||} - 2/g_{\perp} - 2$. According to Hathaway,[37] if the G value is greater than 4, the exchange interaction between the copper centers is negligible, whereas if its value is less than 4 the exchange interaction is noticed. The calculated G-values for the present Cu(II) complexes are 1.116 (**1a**) and 1.366 (**1b**), indicating some interaction between Cu(II) centers in solid complex.[38]

Table 4. Electronic and EPR data of Cu(II) and Ni(II) complexes of ligands **1** and **2**.

Complexes		Electronic spectral data			ESR spectral data			
		λ_{max} in nm (cm^{-1})	Band assignments	Geometry	$g_{\perp}$	$g_{||}$	g_{avg}	G
1a	$[Cu_2(L_1)(Cl)_2(H_2O)_4]$	627.27 (15,942.10)	$^2T_g \leftarrow {}^2E_g$	Distorted	2.392	2.438	2.408	1.116
		393.34 (25,423.30)	L → M	octahedral				
1b	$[Ni_2(L_1)(Cl)_2]$	710.0 (14,084.51)	$^1A_{1g} \rightarrow {}^1E_g$	Square	-	-	-	-
		460.0 (21,739.13)	$^1A_{1g} \rightarrow {}^1B_{2g}$	planar				
2a	$[Cu_2(L_2)(Cl)_2(H_2O)_4]$	630.25 (15,866.72)	$^2T_g \leftarrow {}^2E_g$	Distorted	2.322	2.440	2.361	1.366
		392.88 (25,453.06)	L → M	octahedral				
2b	$[Ni_2(L_2)(Cl)_2]$	710.80 (14,068.66)	$^1A_{1g} \rightarrow {}^1E_g$	Square	-	-	-	-
		460.60 (21,710.81)	$^1A_{1g} \rightarrow {}^1B_{2g}$	planar				

2.6. Thermal studies

The thermal stabilities were investigated for the Cu(II), Ni(II), and Zn(II) complexes of ligand **1** as a function of temperature. The proposed stepwise thermal degradation of the complexes with respect to temperature and the formation of respective metal oxides are given in Table 5. The thermogravimetric curve of Cu(II) complex shows that the complex is stable up to 192 °C and no weight loss occurs before this temperature. The first stage of decomposition represents weight loss of 4 coordinated water molecules and a methyl group at 192.8 °C with practical weight loss of 9.01% (Cald. 8.74%). The resultant complex underwent a second stage of degradation and gave a break at 350 °C with a practical weight loss of 61.39% (Cald. 60.89%), which corresponds to the decomposition of 2 indole moieties ($2C_{15}H_{10}N_2OCl$) and a methyl group. Further, the complex underwent a third stage of decomposition and gave a break at 500 °C with a weight loss of 20.49% (Cald. 19.71%), due to loss of 2 chlorine atoms. Thereafter, the compound showed a gradual decomposition rather than a sharp decomposition up to 800 °C and onwards due to the loss of the remaining organic moiety. The weight of the residue corresponds to 2 moles of cupric oxide.

In the thermogram of the Ni(II) complex, the first stage of decomposition represents the weight loss of 2 Cl_2 molecules at 392 °C with a practical weight loss of 15.16% (Cald. 15.32%). The complex underwent further degradation and gave a break at 550 °C with a practical weight loss of 64.77% (Cald. 64.39%), which corresponds to the decomposition of 2 indole moieties ($2C_{15}H_{10}N_2O$). Thereafter, the compound showed a gradual decomposition up to 850 °C with a weight loss of remaining organic moiety. The weight of the residue corresponds to 2 moles of nickel oxide. In the case of Zn(II) complex, the first stage of decomposition occurs at 342.8 °C with a practical weight loss of 68.15% (Cald. 68.84%), which represents the loss due to 2 indole moieties ($2C_{15}H_{10}N_2OCl$), 2 chlorine atoms, and 2 methyl groups. Thereafter, the compound showed a gradual decomposition up to 800 °C with the weight loss of the remaining organic moiety. The weight of the residue corresponds to 2 moles of zinc oxide. The percentage metal content in all the complexes as done by elemental analysis agrees well with the thermal studies.

Table 5. Thermal data of the complexes of ligand **1**.

Complex No.	Decomposition temp (°C)	% Weight loss		Metal oxide%		Inference
		Obsd	Cald	Obsd	Cald	
1a	192	9.01	8.74	–	–	Loss of coordinated water molecules and CH_3 group
	350	61.39	60.89	–	–	Loss due to 2 indole ($2C_{15}H_{10}N_2OCl$) molecules and CH_3 group
	500	20.49	19.71	–	–	Loss due to 2 chlorine atoms
	Up to 900	–	–	15.98	15.65	Loss due to remaining organic moiety
1b	392	15.16	15.32	–	–	Loss due to 2 chlorine molecules
	550	64.77	64.39	–	–	Loss due to 2 indole ($2C_{15}H_{10}N_2O$) molecules
	Up to 850	–	–	16.38	16.35	Loss due to remaining organic moiety
1c	342	68.15	68.84	–	–	Loss due to 2 indole ($2C_{15}H_{10}N_2OCl$) molecules, 2 chlorine atoms and 2 CH_3 groups.
	Up to 800	–	–	17.07	17.56	Loss due to remaining organic moiety

2.7. Powder X-ray diffraction (XRD) studies

Although the synthesized metal complexes were soluble in some polar organic solvents (DMSO and DMF), crystals that are suitable for single-crystal studies were not obtained. Powder XRD patterns of Cu(II), Ni(II), and Zn(II) complexes of ligand **1** were studied in order to test the degree of crystallinity of the complexes. Powder XRD pattern for Cu(II) complex (**1a**) showed 12 reflections in the range of 3–80° (2θ), which arose from diffraction of X-ray by the planes of complex. The interplanar spacing (d) was calculated by using Bragg's equation, $n\lambda = 2d \sin\theta$. The calculated interplanar d-spacing together with relative intensities with respect to the most intense peak was recorded and is given in Table 6. The unit cell calculations were calculated for cubic symmetry from all the important peaks and $h^2 + k^2 + l^2$ values were determined. The observed interplanar d-spacing values were compared with the calculated ones and they were found to be in good agreement. The $h^2 + k^2 + l^2$ values were 1, 10, 29, 32, 50, 53, 65, 72, 99, 110, 120, and 161. The presence of forbidden number 120 indicates the Cu(II) complex may belong to hexagonal or tetragonal systems.

Table 6. Powder X-ray data of Cu(II) complex of ligand **1**(**1a**).

Peak	2θ	θ	$\sin\theta$	$\sin^2\theta$	1000 $\sin^2\theta$	1000 $\sin^2\theta$/CF ($h^2+ k^2+ l^2$)	hkl	d		a in Å
								Obs	Cal	
1	4.934	2.467	0.0430	0.00184	1.849	1.00(1)	(100)	17.897	17.906	17.90
2	15.716	7.858	0.1367	0.01868	18.68	10.102(10)	(310)	5.634	5.632	17.90
3	26.834	13.417	0.2320	0.05382	53.82	29.107(29)	(520), (432)	3.319	3.318	17.90
4	28.120	14.060	0.2429	0.05900	59.00	31.909(32)	(440)	3.170	3.170	17.90
5	35.506	17.753	0.3049	0.09296	92.96	50.275(50)	(550), (710)	2.526	2.525	17.90
6	36.600	18.300	0.3139	0.09853	98.53	53.288(53)	(641)	2.453	2.453	17.91
7	40.702	20.351	0.3477	0.12089	120.89	65.381(65)	(810)	2.214	2.214	17.92
8	42.821	21.410	0.3650	0.13322	133.22	72.049(72)	(660)	2.110	2.109	17.90
9	50.654	25.327	0.4277	0.18292	182.92	98.929(99)	(933)	1.800	1.800	17.90
10	53.722	26.861	0.4518	0.20412	204.12	110.394(110)	(952)	1.704	1.704	17.90
11	56.131	28.065	0.4704	0.22127	221.27	119.670(120)	–	1.637	1.637	17.90
12	66.179	33.089	0.5459	0.29800	298.00	161.168(161)	(984)	1.410	1.410	17.90

Similar calculations were performed for Ni(II) and Zn(II) complexes of ligand **1**. The Ni(II) complex showed 15 reflections in the range 3–80° (2θ) and the Zn(II) complex showed 7 reflections in the range 0–80° (2θ). The important peaks of both complexes were indexed and the observed interplanar d-spacing values were compared with the calculated ones. The unit cell calculations were performed for a cubic system and the $h^2 + k^2 + l^2$ values were determined for both complexes. The presence of forbidden number 7 for the Ni(II) complex indicates that it may belong to hexagonal or tetragonal systems. Similarly, for the Zn(II) complex, the absence of forbidden numbers (7, 15, 23 etc.) indicates that the complex has cubic symmetry. The calculated lattice parameters were $a = b = c =$ 12.93 Å.

2.8. Electrochemistry

The electrochemical behavior of the Cu(II) complex (**1a**) was investigated in DMF (10^{-3} M) solution containing 0.05 M n-Bu_4N-ClO_4 as a supporting electrolyte by cyclic voltammetry. It is the most versatile electroanalytical technique for the study of electroactive species. The cyclic voltammogram of the Cu(II) complex (**1a**) (Figure 3) in DMF at a scan rate of 50 mV/s shows a well-defined redox process corresponding to the formation of Cu(II)/Cu(I) couple at E_{pa} = –0.5925 V and E_{pc} = –1.0123 V versus Ag/AgCl. The peak separation of this couple is found to be quasi-reversible with ΔE_p = 0.4198 V and the ratio of anodic to cathodic peak height was less than 1. The difference between forward and backward peak potential can provide a rough evaluation of the degree of the reversibility of the one-electron transfer reaction. Thus, the analysis of cyclic voltammetric response to 50 mV/s, 100 mV/s, and 200 mV/s scan rates gives evidence for a quasi-reversible one-electron redox process. The ratio of anodic to cathodic peak height was less than 1 and peak current increases with the increase in the square root of the scan rates, establishing a diffusion-controlled electrode process.[39] From the peak separation value ΔE_p and peak potential increases with higher scan rates, therefore we can suggest that the electrode process is consistent with the quasi-reversibility of the Cu(II)/Cu(I) couple.[40]

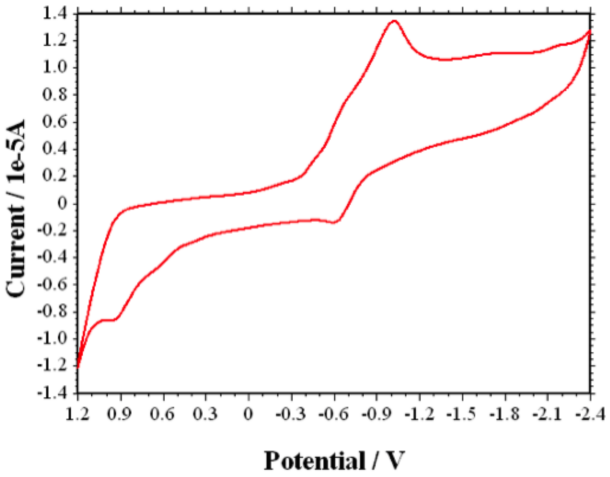

Figure 3. Cyclic voltammogram of Cu(II) complex **(1a)**.

2.9. Pharmacological activity results

2.9.1. In vitro antimicrobial activity

The synthesized ligands **1** and **2**, and their metal complexes were screened for their antimicrobial activity. The antibacterial activity was tested against *E. coli*, *S. typhi*, *B. subtilis*, and *S. aureus* strains and antifungal

activity against *C. albicans*, *C. oxysporum*, and *A. niger* strains. The minimum inhibitory concentration (MIC) values of the compounds against the respective strains are summarized in Table 7. The antimicrobial screening results of all the synthesized compounds exhibited antimicrobial properties, and it is important to note that the metal complexes exhibited a more inhibitory effect compared to their respective parent ligands. The enhanced activity of the complexes over the ligands can be explained on the basis of chelation theory.[41,42] It is known that chelation makes the ligand a more powerful and potent bactericidal agent, thus killing more of the bacteria than the ligand. The enhancement in the activity may be rationalized on the basis that ligands mainly possess an azomethine (C = N) bond. It has been suggested that ligands with hetero donor atoms (nitrogen and oxygen) inhibit enzyme activity, since the enzymes that require these groups for their activity appear to be especially more susceptible to deactivation by metal ions on coordination. It is observed that, in a complex, the positive charge of the metal ion is partially shared with the hetero donor atoms (nitrogen and oxygen) present in the ligand, and there may be π-electron delocalization over the whole chelating system.[43,44] Thus the increase in the lipophilic character of the metal chelates favors their permeation through the lipoid layer of the bacterial membranes and blocking of the metal binding sites in the enzymes of microorganisms. Other factors, namely solubility, conductivity, and bond length between the metal ion and the ligand, also increase the activity. The increase in the activity of metal complexes against fungi is due to the formation of a hydrogen bond between the azomethine nitrogen atom and active centers of the cell constituents, resulting in interference with the normal cell process.

Table 7. Minimum inhibitory concentration (MIC μg mL^{-1}) of ligands and their metal complexes.

Compound	Zone of inhibition against bacteria (mm)				Zone of inhibition against fungi (mm)		
	E. coli	*S. aureus*	*B. subtilis*	*S. typhi*	*C. albicans*	*C. oxysporum*	*A. niger*
1	50	75	50	100	75	50	50
1a	12.50	25	25	50	25	12.50	12.50
1b	25	50	12.50	50	12.50	25	25
1c	12.50	25	25	50	25	12.50	25
2	50	50	75	75	25	12.50	25
2a	12.50	12.50	12.50	25	12.50	25	12.50
2b	25	12.50	25	50	25	25	12.50
2c	25	25	25	50	12.50	25	25
Gentamicin	12.50	12.50	12.50	12.50	-	-	-
Fluconazole	-	-	-	-	12.50	12.50	12.50

2.9.2. DNA cleavage activity

Ligand **1** and its Cu(II), Ni(II), and Zn(II) complexes, and ligand **2** and its Cu(II) complex were studied for their DNA cleavage activity by agarose gel electrophoresis against calf-thymus DNA (Cat. No. 105850) and the gel picture showing cleavage is depicted in Figure 4.

DNA-cleavage studies are used for rational design and to construct new and more efficient drugs that are targeted to DNA.[45] The cleavage efficiency of all the compounds compared to the control is due to their efficient DNA-binding ability, which is observed by diminishing of the intensity of the lanes. The DNA-cleavage study by electrophoresis analysis clearly revealed that the lane ligand **1** and its Zn(II) complex showed partial cleavage, whereas lane Cu(II) and Ni(II) complexes of ligand **1**, ligand **2** and its Cu(II) complex showed complete cleavage of DNA. The difference was observed in the bands of lanes of compounds compared with the control DNA of calf-thymus. This shows that the control DNA alone does not show any apparent cleavage, whereas the ligands

and metal complexes do. The result indicates the important role of the coordination of nitrogen and oxygen to the metal ion in these isolated DNA cleavage reactions. On the basis of the cleavage of DNA observed in the case of ligands **1** and **2** and their Cu(II) and Ni(II) and Zn(II) and Cu(II) complexes, respectively, it can be concluded that all the compounds in the present study inhibit the growth of pathogenic organism by DNA cleavage as was observed on the DNA cleavage of calf-thymus.

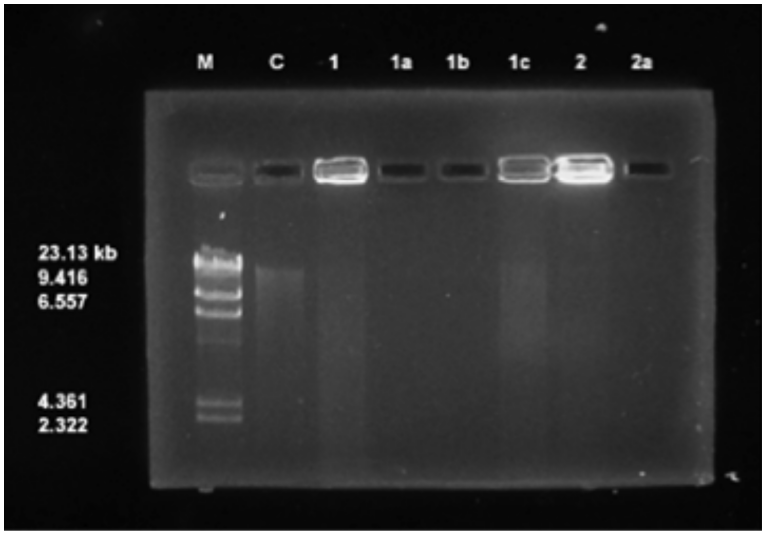

Figure 4. DNA cleavage of calf-thymus DNA. **M**, standard molecular weight marker; **C**, control. Lane **1**, **1a**, **1b**, **1c**, **2,** and **2a** were treated DNA of calf-thymus DNA genome with respective compounds.

Based on these studies, the newly synthesized binuclear ligands and their complexes were characterized by various spectral studies and analytical data. The coordinating ability of the ligands was proved in complexation reactions with Cu(II), Ni(II), and Zn(II) ions. In all the complexes both ligands act as a tridentate chelate around the metallic ion with 2 compartments and provide ONO donating sites to each metal ion in both compartments. Cu(II) complexes of both ligands have octahedral geometry, whereas Ni(II) and Zn(II) complexes of both the ligands possess square planar and tetrahedral geometries, respectively. The Cu(II) complex of ligand **1** exhibits one-electron transfer quasi-reversible redox activity in the applied potential range. The antimicrobial activity results show that all the complexes exhibited higher activity when compared to their respective ligands. The DNA cleavage studies revealed that the metal complexes showed good efficiency towards DNA cleavage. Based on the analytical data and spectral studies, the proposed structures of all the complexes are depicted in Figure 5.

3. Experimental

3.1. Analysis and physical measurements

IR spectra of the newly synthesized compounds were recorded as KBr pellets on a PerkinElmer FT-IR instrument in the region 4000–350 cm^{-1}. ^1H NMR spectra of the Zn(II) complexes were recorded in d_6-DMSO using a Bruker DRX-400 MHz instrument. UV-visible spectra of the Cu(II) and Ni(II) complexes were recorded on an Elico-SL 164 double beam spectrometer in the range 200–1000 nm in DMF solution (1×10^{-3} M). Elemental analysis was obtained from a HERAEUS C, H, N-O rapid analyzer and metal analysis was carried out by following the standard methods. ESI-MS was recorded on an Agilent 6330 Ion trap-mass spectrophotometer.

ESR measurements of Cu(II) complexes in polycrystalline state were obtained on a BRUKER Bio Spin Gmbh spectrometer at a microwave frequency of 9.903 GHz. The experiment was carried out by using DPPH as reference with the field set at 3950 G. Electrochemistry of the Cu(II) complex was recorded on a 600 D series model electrochemical analyzer in DMF using n-Bu_4N-ClO_4 as a supporting electrolyte. Powder-XRD of the complexes was recorded using a Bruker AXS D8 Advance (Cu, wavelength 1.5406 Å source). Molar conductivity measurements were recorded on an ELICO CM-180 conductivity bridge in dry DMF (10^{-3} M) solution using a dip-type conductivity cell fitted with a platinum electrode, and the magnetic susceptibility measurements were made at room temperature on a Gouy balance using $Hg[Co(NCS)_4]$ as the calibrant.

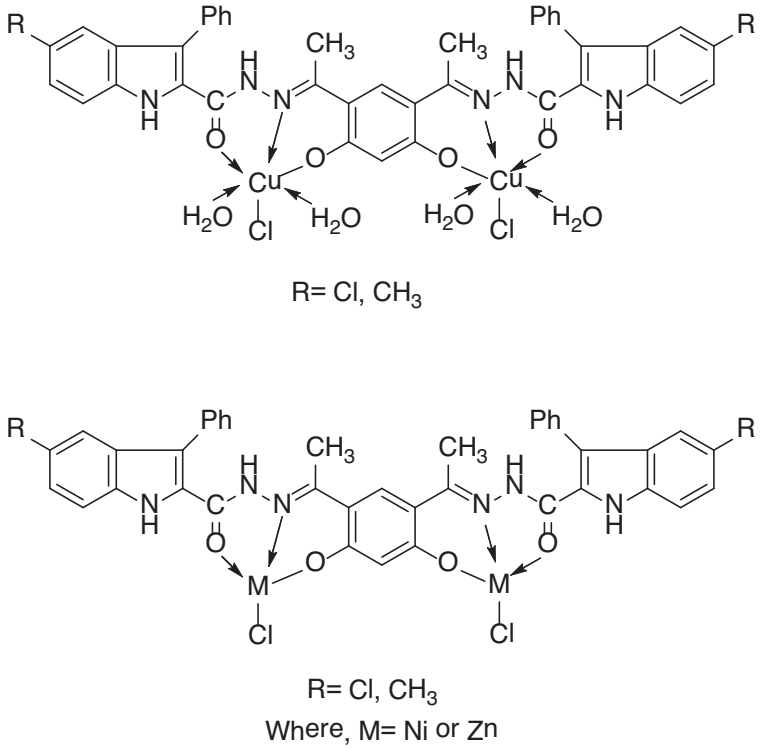

Figure 5. Suggested structure for Cu(II), Ni(II), and Zn (II) of ligand **1** and **2**.

3.2. Methods

All the chemicals used were of reagent grade and procured from Hi-media and Sigma Aldrich. The solvents were dried and distilled before use. Melting points of the newly synthesized compounds were determined by electro-thermal apparatus using open capillary tubes. The metal and chloride contents of the metal complexes were determined as per standard procedures.[46] 5-Substituted-3-phenyl-*1H*-indole-2-carboxyhydrazide was prepared by the literature method.[47] The 4,6-diacetyl resorcinol was procured from Sigma Aldrich.

3.2.1. Synthesis of ligands 1 and 2

A mixture of 5-substituted-3-phenyl-*1H*-indole-2-carboxyhydrazide (0.002 mol) and 4,6-diacetylresorcinol (0.001 mol) with a catalytic amount of glacial acetic acid (1–2 drops) in ethanol (20 mL) was refluxed on a water bath for about 7–8 h. The reaction was monitored by TLC. The pale yellow colored solid separated was filtered, washed with a little ethanol, dried, and recrystallized from dioxane (Scheme 5).

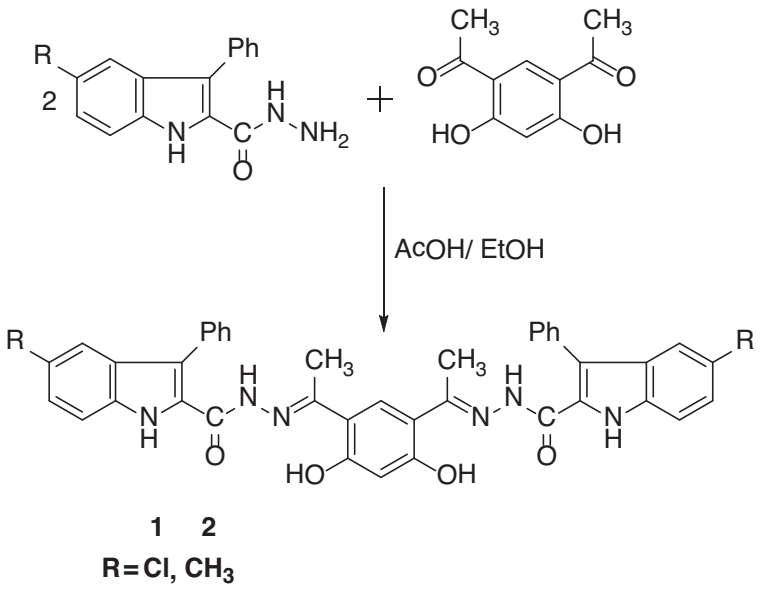

Scheme 5. Synthesis of ligands **1** and **2**.

Mol. For. = $C_{40}H_{30}N_6O_4Cl_2$, mp = 305 °C, yield = 71% (Schiff base **1**)
Mol. For. = $C_{42}H_{36}N_6O_4$, mp = 310 °C, yield = 68% (Schiff base **2**)

3.2.2. Synthesis of Cu(II), Ni(II), and Zn(II) complexes of Schiff bases 1 and 2

To a hot solution of 5-substituted-*N*'-(1-(5-1-(2-(5-substituted-3a,7a-dihydro-1*H*-indole-2-carbonyl)hydrazono)ethyl)-2,4-dihydroxyphenyl)ethylidene)-1*H*-indole-2-carbohydrazide (**1** and **2**) (0.001 mol) in ethanol (30 mL) was added a hot ethanolic solution (15 mL) of respective metal chlorides (0.002 mol). The reaction mixture was then refluxed on a water bath for about 4–5 h. An aqueous alcoholic solution of sodium acetate (0.5 g) was added to the reaction mixture to maintain a neutral pH and refluxing was continued for about 1 h more. The reaction mixture was poured into distilled water and the separated solid complexes were collected by filtration, washed with a sufficient quantity of distilled water, then with hot ethanol to apparent dryness, and dried in a vacuum over anhydrous calcium chloride in a desiccator.

3.3. Pharmacological activity

3.3.1. Antimicrobial assays

The biological activities of the synthesized Schiff bases **1** and **2** and their Cu(II), Ni(II), and Zn(II) complexes were studied for their antibacterial and antifungal activities by the disk and well diffusion methods, respectively. The in vitro antibacterial activities of the compounds were tested against 2 gram-negative (*E. coli* and *S. typhi*) and 2 gram-positive (*B. subtilis* and *S. aureus*) bacteria. The in vitro antifungal activities were tested against *C. albicans*, *C. oxysporum*, and *A. niger*.[48,49] Stock solutions of the test chemicals (1 mg mL^{-1}) were prepared by dissolving 10 mg of each test compound in 10 mL of distilled DMSO solvent. Different concentrations of the test compounds (100, 75, 50, 25, and 12.5 μg mL^{-1}) were prepared by diluting the stock solution with the required amount of distilled DMSO. Further, the controlled experiments were carried out by using DMSO solvent alone.

3.3.2. Antibacterial screening

Mueller–Hinton agar medium was used for the antibacterial studies. The pure dehydrated Mueller–Hilton agar (38 g) was dissolved in 1000 mL of distilled water. Pure cultures of the bacterial strains *E. coli*, *S. aureus*, *B. subtilis*, and *S. typhi* were subcultured by inoculating in the nutrient broth and they were incubated at 37 °C for about 18 h. The agar plates were prepared by using the above Mueller–Hinton agar medium and wells were dug with the help of a 6-mm sterile metallic cork borer. Each plate was inoculated with an 18-h-old bacterial culture (100 μL) using a micropipette and spread uniformly using a bent glass rod on each plate. The drug gentamicin was used as standard. Different concentrations of the test compounds were incorporated into the wells using a micropipette and the plates were incubated at 37 °C for 24 h. Soon after the completion of the incubation period, the diameter of the inhibition zone generated by each test compound against bacterial growth was measured using an antibiogram zone measuring scale.

3.3.3. Antifungal screening

Potato dextrose agar (PDA) medium was used for the antifungal studies. The following ingredients were used to prepare the medium: potatoes (sliced, washed, unpeeled) 200 g, dextrose 20 g, agar 20 g in 1000 mL of distilled water. Pure cultures of *C. albicans*, *C. oxysporum*, and *A. niger* were inoculated on PDA slants. These slants were incubated at 32 °C for 7 days. To these 7-day-old slants of fungal strains, 10 mL of 0.1% Tween-80 solution was added and the cultures were scraped with a sterile inoculating loop to get uniform spore suspension. The agar plates were prepared using the above PDA medium and wells were dug with the help of a 6-mm sterile metallic cork borer. Each plate was inoculated with a 7-day-old spore suspension of each fungal culture (100 μL) using a micropipette and spread uniformly using a bent glass rod on each plate. Each well was incorporated with the test compound solution of different concentrations. The drug fluconazole was used as standard. All the inoculated plates were incubated at 32 °C for about 48 h. Soon after the completion of the incubation period the diameter of the inhibition zone generated by each test compound against fungal growth was measured using an antibiogram zone measuring scale.

3.3.4. DNA cleavage experiment

The extent to which the newly synthesized ligands and their metal complexes could function as DNA cleavage agents was examined using calf-thymus DNA (Cat. No. 105850) as a target. Electrophoresis was employed to study the efficiency of cleavage by the synthesized compounds. Nutrient broth medium was used (Peptone 10 g, NaCl 10 g, and yeast extract 5 g L^{-1}) for culturing calf-thymus. The electrophoresis of the test compounds was done according to the literature method.[50]

The freshly prepared calf-thymus culture (1.5 mL) was centrifuged, and the pellets obtained were then dissolved in 0.5 mL of lysis buffer (50 mM EDTA, 100 mM Tris pH 8.0, 50 mM lysozyme). To this, 0.5 mL of saturated phenol was added and the resulting mixture was incubated at 55 °C for 10 min. Soon after the incubation the solution was centrifuged at 10,000 rpm for 10 min and to the supernatant liquid an equal volume of chloroform:isoamyl alcohol (24:1) and 1/20 volume of 3 M sodium acetate (pH 4.8) were added. Again the solution was centrifuged at 10,000 rpm for 10 min and the supernatant layer was collected and then mixed with 3 volumes of chilled absolute alcohol, and the DNA precipitates. The precipitated DNA was separated by centrifugation and the pellet was dried and dissolved in Tris buffer (10 mM Tris pH 8.0) and stored in cold conditions.

Agarose (250 mg) was dissolved in hot Tris–acetate–EDTA (TAE) buffer (25 mL) (4.84 g Tris base, pH 8.0, 0.5 M EDTA L^{-1}) and heated to boil for a few minutes. When the gel was approximately 55 °C, it was poured into a gas cassette fitted with a comb. Slowly the gel was allowed to solidify by cooling to room temperature and then carefully the comb was removed. The solidified gel was placed in the electrophoresis chamber containing TAE buffer. Test compounds (1 mg mL^{-1}) were prepared in DMSO. The test compounds (25 μg) were added to the isolated DNA of calf-thymus and they were incubated for 2 h at 37 °C. Soon after the incubation period the DNA sample (20 μL) was mixed with bromophenol blue dye in equimolar ratio and along with standard DNA marker containing TAE buffer was loaded carefully into the wells and a constant 50 V of electricity was supplied for about 30 min. Later, the gel was removed and stained with ethidium bromide solution (0.01 M) for 15–20 min and then the bands were observed and photographed under a UV-illuminator.

Acknowledgements

The authors are grateful to the Professor and Chairman, Department of Chemistry, Gulbarga University, Gulbarga, for providing the laboratory facilities. We also thank SAIF, STIC Cochin University, Chairman, Department of Material Science Gulbarga University, Gulbarga, for providing spectral data, and BioGenics Research and Training Centre in Biotechnology, Hubli, for biological activities.

References

1. Chavan, R. S.; More, H. N.; Bhosale, A. V. *Torpical J. Pharm. Res.* **2011**, *10*, 463–473.
2. Misra, U.; Hitkari, A.; Saxena, A. K.; Gurtu, S.; Shanker, K. *Eur. J. Med. Chem.* **1996**, *31*, 629–634.
3. Preeti, R.; Srivastava, V. K.; Ashok, K. *Eur. J. Med. Chem.* **2004**, *39*, 449–452.
4. El-Gendy Adel, A.; Abdou Naida, A.; Sarhan El-Taher, Z.; El-Banna Hosney, *A. Alexandria J. Pharma. Sci.* **1993**, *7*, 99–103.
5. Dandia, A.; Sehgal, V.; Singh, P. *Indian J. Chem.* **1993**, *32B*, 1288–1291.
6. Kalgutkar, A. S.; Crews, B. C.; Saleh, S.; Prudhomnae, D.; Marnett, L. *J. Bioorg. Med. Chem.* **2005**, *13*, 6810–6822.
7. Sureyya, O.; Dogu, N. *I. L. Farmaco.* **2002**, *57*, 677–683.
8. Leneva, I. A.; Fadeeva N. I.; Fedykina, I. T. Abstract 187, In *7th International Conference on Antiviral Research,* 1994.
9. Ergenc, N.; Gunay, N. S.; Demirdamar, R. *Eur. J. Med. Chem.* **1998**, *33*, 143–148.
10. Louis. H. A. P.; Jacobas, P. P.; Sarel, F. M. *Eur. J. Med. Chem.* **2010**, *45*, 4458–4466.
11. Merwade, A. Y.; Rajur, S. B.; Basngoudar, L. D. *Indian J. Chem.* **1990**, *29B*, 1113–1117.
12. Fernandez, A. E.; Monge, V. A. Span. Pat. 400, 436. Chem Abstract 1975, 83, 1142059.
13. Gangadharmath, U. B.; Revankar, V. K.; Mahale, V. B. *Spectrochim. Acta. Part A.* **2002**, *58*, 2651–2657.
14. Seleem, H. S.; El-Shetary, B. A.; Khalil, S. M. E.; Mostafa, M.; Shebl, M. *J. Coord. Chem.* **2005**, *58*, 479–493.
15. Shebl, M. *Spectrochim. Acta. Part A.* **2009**, *73*, 313–323.
16. Liu, S. L.; Wen, C. L.; Qi, S. S.; Liang, E. X. *Spectrochim. Acta. Part A.* **2008**, *69*, 664–669.
17. Taha, A. *Spectrochim. Acta. Part A.* **2003**, *59*, 1611–1620.
18. Seleem, H. S.; El-Shetary, B. A.; Shebl, M. *Heteroatom. Chem.* **2007**, *18*, 100–107.
19. Solomon, E. I. *Pure Appl. Chem.* **1983**, *55*, 1069–1088.
20. Niederhoffer, C. E.; Tommons, J. H.; Martell, A. G. *Chem. Rev.* **1984**, *84*, 137–203.

21. Jadegoud, Y.; Ijare, O. B.; Mallikarjuna, N. N.; Angandi, S. D.; Mruthyunjayaswamy, B. H. M. *J. Indian Chem. Soc.* **2002**, *79*, 921–924.
22. Mruthyunjayaswamy, B. H. M.; Ijare, O. B.; Jadegoud, Y. *J. Brazilian Chem.* Soc. **2005**, *16*, 783–789.
23. Mruthyunjayaswamy, B. H. M.; Jadegoud, Y.; Ijare, O. B.; Patil, S. G.; Kudari, S. M. *Trans. Metal Chem.* **2005**, *30*, 234–242.
24. Rahaman, F.; Ijare, O. B.; Jadegoud, Y.; Mruthyunjayaswamy, B. H. M. *J. Coord. Chem.* **2009**, *1*, 1–11.
25. Geary, W. J. *Coord. Chem. Rev.* **1971**, *7*, 81–122.
26. Roy, S.; Mandal, T. N.; Das, K.; Butcher, R. J.; Rheingold, A. L.; Kar, S. K. *J. Coord. Chem.* **2010**, *63*, 2146–2157.
27. Sulekha; Lokesh, K. G. *Spectrochim. Acta. Part A.* **2005**, *61A*, 269–272.
28. Dholakiya, P. P.; Patel, M. N. *Synth. React. Inorg. Metal-Org. Chem.* **2002**, *32*, 753–762.
29. Liu, H.; Wang, H.; Gao, F.; Niu, D.; Lu, Z. *J. Coord. Chem.* **2007**, *60*, 2671–2678.
30. Koji, A.; Kanako, M.; Ohba, M.; Okawa, H. *Inorg. Chem.* **2002**, *41*, 4461– 4467.
31. Azza, A. A. A. *J. Coord. Chem.* **2006**, *59*, 157–176.
32. Mishra, A. P.; Mishra, R. K.; Shrivastava, S. P. *J. Serb. Chem. Soc.* **2009**, *74*, 523–535.
33. Shriver, D. F.; Atkins, P. W.; Langford, C. H. *Inorganic Chemistry*, Oxford University Press: Oxford, 1990, pp. 434–468.
34. Balasubramanian, S.; Krishnan, C. N. *Polyhedron* **1986**, *5*, 669–679.
35. Speier, G.; Csihony, J.; Whalen, A. M.; Pierpont, C.G. *Inor. Chem.* **1996**, *35*, 3519–3524.
36. Kilveson, D. *J. Phys. Chem. B.* **1997**, *101*, 8631–8634.
37. Hathaway, B. J.; Billing, D. E. *Coord. Chem. Rev.* **1970**, *5*, 143–207.
38. Bencini, A.; Gattechi, D. *EPR of Exchange Coupled System*; Springer-Verlag: Berlin, 1990.
39. Bard, A. J.; Faulkner, L. R. *Electrochemical Methods;* 2nd ed. Wiley. New York, 2001.
40. Patil, S. A.; Naik, V. H.; Kulkarni, A. D.; Badami, P. S. *J. Sulphur Chem.* **2010**, *31,* 109–121.
41. Chohan, Z. H.; Arif, M.; Akhtar, M. A.; Supuran, C. T. *Bioinorg. Chem. Appl.* **2006**, 1–13.
42. Thimmaiah, K. N.; Lioyd, W. D.; Chandrappa, G. T. *Inorg. Chim. Acta.* **1985**, *160*, 81–85.
43. Wahab, Z. H. A.; Mashaly, M. M.; Salman, A. A.; El-Shetary, B. A.; Faheim, A. A. *Spectrochim. Acta. Part A.* **2004**, *60*, 2861–2864.
44. Meyer, B. N.; Ferrigni, N. R.; Putnam, J. E.; Jacobsen, L. B.; Nichols, D. E.; McLaughlin, J. L. *Planta Med.* **1982**, 45, 31–34.
45. Waring, M. J. *Drug Action at the Molecular Level;* Roberts, G. C. K. Ed, Macmillan: London, 1977.
46. Vogel, A. I. *A Text Book of Quantitative Inorganic Analysis*; 3rd edn. Longman ELBS, London, 1968.
47. Hiremath, S. P.; Mruthyunjayaswamy, B. H. M.; Purohit, M. G. *Indian J. Chem.* **1978**, *16B*, 789–792.
48. Walker, R. D. Antimicrobial susceptibility testing and interpretation of results. In J. F. Prescott, J. D. Baggot & R. D. Walker, (Eds.), *Antimicrobial Therapy in Veterinary Medicine.* Ames, IA, Iowa State University Press. 2000. pp. 12–26.
49. Sadana, A. K.; Miraza, Y.; Aneja, K. R.; Prakash, O. *Eur. J. Med. Chem.* **2003**, 38, 533–536.
50. Sambrook, J.; Fritsch, E. F.; Maniatis, T. *Molecular Cloning, A Laboratory Manual*; 2nd edn. Cold Spring Harbor Laboratory, Cold Spring Harbor, New York, 1989.